JOURNAL OF VIROLOGY, Oct. 1996, p. 6947–6954 Vol. 70, No. 10
0022-538X/96/$04.00+0

Selective Transmission of Human Immunodeficiency Virus Type 1 Variants to SCID Mice Reconstituted with Human Peripheral Blood Mononuclear Cells

RICHARD B. MARKHAM,[1]* DAVID H. SCHWARTZ,[1] ALAN TEMPLETON,[2] JOSEPH B. MARGOLICK,[1] HOMAYOON FARZADEGAN,[3] DAVID VLAHOV,[3] AND XIAO-FANG YU[1]

Departments of Molecular Microbiology and Immunology[1] and Epidemiology,[3] Johns Hopkins School of Hygiene and Public Health, Baltimore, Maryland, and Department of Biology, Washington University, St. Louis, Missouri[2]

Received 8 March 1996/Accepted 17 July 1996

The relative infectiousness of laboratory and primary human immunodeficiency virus type 1 (HIV-1) variants was evaluated in in vitro cell cultures of peripheral blood mononuclear cells or MT-2 cells and in Hu-PBL-SCID mice. HIV_{MN} and syncytium-inducing primary isolates were preferentially transmitted to cells in tissue culture. HIV_{Ba-L} and non-syncytium-inducing (NSI) primary isolates were more infectious in Hu-PBL-SCID mice. Phylogenetic analysis of *env* sequences derived from the primary isolates, from the cell cultures, and from five Hu-PBL-SCID mice was performed by using methods designed for resolving differences among closely related sequence pairs. This analysis demonstrated preferential transmission of an evolutionarily related subset of NSI variants to Hu-PBL-SCID mice. The pattern of selective transmission of a restricted range of NSI variants that is observed in the clinical setting is maintained in Hu-PBL-SCID mice and not in tissue culture systems. The Hu-PBL-SCID mouse model system, when used with appropriate phylogenetic analysis methodologies, will be useful for identifying and characterizing the more infectious HIV-1 variants that should be targeted for vaccine development.

Individuals infected with human immunodeficiency virus type 1 (HIV-1) for many years typically carry many genetic variants of the virus (5, 8, 10, 15). Despite their presumed exposure to such a diverse array of viral variants, recently infected individuals acquire a remarkably restricted range of non-syncytium-inducing (NSI) variants of the virus, which often represent minority populations of those viruses carried in the individual from whom the infection was acquired (11, 14, 30, 31). The apparent viral selection which occurs in the newly infected host could depend on unique properties of the infecting virus, host factors that differ between the established host and the naive individual, or both. To explore the basis for this selection, we have examined the abilities of different viral variants to establish infection in two different cellular environments: standard human peripheral blood mononuclear cell (PBMC) tissue culture and mice with severe combined immunodeficiency that have been reconstituted with human PBMC (Hu-PBL-SCID mice).

These two environments were selected for study because of the possibility that the cells in culture might be more activated than those in Hu-PBL-SCID mice. Standard culture of HIV-1 requires that PBMC be initially stimulated with the T-cell mitogen phytohemagglutinin (PHA) and then maintained in interleukin-2, which preserves the activated state. In Hu-PBL-SCID mice, on the other hand, human T cells are not directly stimulated before being placed in the mice, yet HIV-1 infection can be readily established (16, 17, 22, 23). Because it has been proposed that T-cell activation is critical for productive infection in vitro (2, 29), we hypothesized that T cells in these two environments might be differentially activated at the time of viral infection and that the range of viruses that could establish infection might, therefore, be different. In this study we evaluated this hypothesis by inoculating standard PBMC cultures and Hu-PBL-SCID mice with different laboratory and primary variants of HIV-1. An evolutionary comparison of Env sequences from the source virus and from the transmitted viruses was then used to determine the relative infectiousness of different variants and phylogenetically related sets of variants in the distinct settings.

These evolutionary analyses make use of a recent phylogenetic estimation algorithm (25) designed specifically for closely related sequences. The utility and power of this phylogenetic estimation procedure, which differs from the frequently used maximum parsimony procedure (4, 20), has already been demonstrated in an analysis of Florida dentist-patient viral sequences (3), and is likewise needed here because of the close similarity of many of our sequences. This type of analysis also takes into account both the possibility that population genetic data may not be strictly bifurcating and that recombination may occur (3).

MATERIALS AND METHODS

Mice. Male and female CB.17 *scid/scid* mice between 4 and 6 weeks of age were obtained from a breeding colony maintained at the Johns Hopkins Medical Institutions. Prior to viral inoculation, mice were reconstituted by intraperitoneal injection with 2×10^7 Ficoll-Hypaque-purified (Sigma Chemical Co., St. Louis, Mo.) PBMC obtained by hemapheresis of a healthy HIV-seronegative individual. Eight days later mice with circulating human immunoglobulin (IgG) concentrations greater than 5 μg/ml, as determined by standard enzyme-linked immunosorbent assay, were inoculated with the indicated doses of the various HIV-1 strains. Mouse usage was in accordance with protocols approved by the institutional Animal Care and Use Committee.

Virus. HIV-1 strains HIV_{Ba-L} and HIV_{MN} were obtained from Advanced Biotechnologies (Columbia, Md.). The primary virus isolate represents a mixture of viral variants obtained from a 10-day coculture of PBMC from an HIV-infected subject and from a healthy, HIV-seronegative individual. The PBMC from the healthy subject had been prestimulated with PHA and cultured in the presence of interleukin-2. The unfiltered supernatant from that culture was used to inoculate other cultures or Hu-PBL-SCID mice. The subject who served as a source of the virus was a participant in the AIDS Linked to the Intravenous Experience (ALIVE) cohort of injecting drug users from Baltimore, Md., mon-

* Corresponding author. Mailing address: Department of Molecular Microbiology and Immunology, Johns Hopkins School of Public Health, 615 N. Wolfe St., Baltimore, MD 21205. Phone: (410) 955-9601. Fax: (410) 558-1250.

itored at the Johns Hopkins School of Hygiene and Public Health. This culture supernatant fluid was selected on the basis of unpublished data indicating that it contained a heterogeneous virus population.

Quantitation of virus inoculated into Hu-PBL-SCID mice and recovered from tissue culture. Fifty-percent tissue culture infective doses were determined for strains HIV_{Ba-L} and HIV_{MN} by determining titers either on the H9 T-cell line (HIV-1_{MN}) or on primary macrophages (HIV_{Ba-L}).

The relative abilities of HIV_{MN} and HIV_{Ba-L} to establish infection in human PBMC tissue culture were determined by using PBMC from the same source as that used in the Hu-PBL-SCID mouse studies. For in vitro culture, these cells were stimulated with PHA (1 μg/ml) (Life Sciences, Inc., Grand Island, N.Y.) for 2 days and subsequently maintained in media supplemented with interleukin-2 (2 U/ml) (Pharmingen, Indianapolis, Ind.). Growth of virus from the cultures was determined by assay for viral p24 antigen (Abbott Diagnostics, Abbott Park, Ill.) 10 days after culture initiation.

Virus recovery from Hu-PBL-SCID mice. To determine whether HIV_{MN} or HIV_{Ba-L} had established infection in the Hu-PBL-SCID mice at given inocula, cells were harvested from the mice by peritoneal lavage 2 weeks after viral inoculation and 5×10^5 cells were subjected to virus strain-specific PCR. The primers used to amplify HIV_{MN} were 5′-GAAGAGGTAGTAATTAGATCTGAG and 3′-TCTGGGTCCCCTCCTGAGGATTGA. These primers amplify the region between bases 7055 and 7356 of the HIV_{MN} genome, which is located in the *env* gene. The primers used to amplify HIV_{Ba-L} were from the same region of that virus and were 5′-GAAGAGGTAGTAATTAGATCCGCC and 3′-TCTGGGTCCCCTCCTGAGGAGTGC. The underlined portions of the primers indicate the four terminal bases which were the only bases that differed between the corresponding HIV-1_{MN} and HIV_{Ba-L} primers. Preliminary experiments indicated that the HIV-1_{MN} primers did not produce an amplification product when tested against an HIV_{Ba-L} template and vice versa. The PCR was run for 2 min at 95°C, followed by 35 cycles of 94°C for 30 s, 60°C for 30 s, and 72°C for 45 s.

Cloning and sequencing. Nested PCR was used to amplify a region of the *env* gene from the cultured cells, from peritoneal cells harvested from Hu-PBL-SCID mice, or from cDNA obtained by reverse transcribing viral RNA present in supernatant fluid from the primary culture of the subject's PBMC. Reverse transcription was performed according to the manufacturer's instructions (cDNA Cycle kit; Invitrogen Corporation, San Diego, Calif.). The external *env* primers used were 5′-GTCAGCACAGTACAATGTACACATG (nucleotides 6947 to 6971, based on sequence numbering in the molecular clone HXB2) and 5′-AATTACAGTAGAAAAATTCCCCTC (nucleotides 7359 to 7382 of HXB2), and the nested primers were 5′-CGGGATCCTGTTAAATGGCAGTCTAGCAGAAG (nucleotides 7002 to 7025 of HXB2) and 5′-CGGAATTCCGTTACAATTTC-TGGGTCCCCTCC (nucleotides 7319 to 7342 of HXB2). The underlined portions of the primers are, respectively, *Bam*HI or *Eco*RI restriction sites included in the nested primers for cloning purposes. Both first- and second-round PCRs were run for 2 min at 95°C, followed by 35 cycles of 94°C for 30 s, 60°C for 30 s, and 72°C for 45 s. At the end of the 35 cycles the samples were held at 72°C for 10 min before returning to the 4°C temperature, at which they were held until further analysis. The amplified sequences from the nested PCR were then cloned into pUC19 by standard methods (13) and sequenced by the Sanger chain termination method (21) with the appropriate nested primers described above. A total of 96 clones were sequenced for this analysis.

Phylogenetic analysis. The methods by which the evolutionary network was established and the statistical analysis that was applied to determine the significant associations within the network are described in Appendix.

Flow-cytometric analysis. Preliminary experiments indicated a low proportion of human cells among the peritoneal exudate cells of the mice. Therefore, the peritoneal cells were enriched for human cells by negative selection of mouse cells using the panning method described by Wysocki and Sato (28). Briefly, 3×10^7 peritoneal cells harvested from mice were placed on a petri dish that had been previously coated with a monoclonal antibody specific for mouse H-$2K^d$ for 60 min at 4°C. Aliquots of the nonadherent cells were then stained with monoclonal antibodies conjugated to fluorescein isothiocyanate (FITC), phycoerythrin (PE), and PE-cyanine 5 (Cy5) in the following combinations: (i) IgG1-FITC, IgG2a-PE, and IgG1-Cy5 as an isotype control tube, (ii) anti-human CD45-FITC and anti-mouse H-$2K^d$-PE to identify proportions of human and mouse leukocytes, respectively, (iii) anti-human CD4-FITC, mouse IgG_2-PE, and anti-human CD3-Cy5 to define the boundary between HLA-DR^+ and HLA-DR^- human $CD4^+$ T cells, and (iv) anti-human CD4-FITC, anti-HLA-DR-PE, and anti-human CD3-Cy5 to identify human T ($CD3^+$) cells expressing both CD4 and HLA-DR. All antibodies, and their isotype controls, were obtained from BDIS (San Jose, Calif.) except for Cy5 conjugates (Caltag, South San Francisco, Calif.) and H-$2K^d$ (Pharmingen, San Diego, Calif.).

Analyses were performed on an ELITE flow cytometer (Coulter Electronics, Hialeah, Fla.). Lymphocytes were gated on the basis of forward and 90° light scatter characteristics which were confirmed in each experiment by verifying the light scatter characteristics of all cells expressing CD45 or H-$2K^d$ (i.e., "back-gating"). Analysis of human T cells was gated on CD3 expression, and the nonspecific binding of IgG_2-PE (0 to 1% of the cells) was subtracted from the proportion of cells that stained positive for HLA-DR-PE in tube 4. Results were expressed as percentage of human $CD4^+$ T cells that coexpressed HLA-DR. The number of gated lymphocytes counted in each experiment was between 5,000 and 10,000.

TABLE 1. Relative abilities of HIV-1_{MN} and HIV_{Ba-L} to establish infection in tissue cultures containing PHA- and interleukin-2-activated PBMC[a]

No. of $TCID_{50}$s	p24 OD	
	HIV_{MN}	HIV_{Ba-L}
10^2	0.25	0.05[b]
10^3	1.30	0.16
10^4	>2.0	1.54

[a] $TCID_{50}$, 50% tissue culture infective dose; OD, optical density.
[b] The value is less than that for the negative control.

RESULTS

Relative infectiousness of SI and NSI variants of HIV-1 in PHA-stimulated PBMC tissue culture and Hu-PBL-SCID mice. Two distinct HIV-1 variants were tested for their relative infectiousness in tissue culture systems and in Hu-PBL-SCID mice: HIV-1_{MN}, which does not grow well in macrophages and which induces syncytia when cultured with certain T-cell lines (a syncytium-inducing [SI] variant), and HIV_{Ba-L}, an NSI variant that grows well in macrophages.

To control for potential variation among different Hu-PBL-SCID mice, the two viruses were mixed at equal 50% tissue culture infectious doses and the mixture was inoculated into Hu-PBL-SCID mice at serial tenfold dilutions. In the mice, HIV-1_{Ba-L} established infection at a 2-log-lower inoculum than HIV_{MN} (10^2 versus 10^4 50% tissue culture infective doses). In contrast, when the individual viruses were inoculated separately into PHA-stimulated PBMC tissue cultures that used the same source of human cells, HIV_{MN} established infection at a 1-log-lower concentration than HIV_{Ba-L} (Table 1). With human PBMC from the same subject, these two viruses therefore differed in their relative levels of infectiousness for Hu-PBL-SCID mice and PBMC tissue culture.

In a second experiment, using cells from a different subject to both reconstitute SCID mice and establish tissue culture, a 2-log increase in infectiousness of HIV-1_{Ba-L} compared with HIV_{MN} was again observed. In this experiment the two viruses were essentially equivalently infectious in tissue culture (data not shown).

Relative infectiousness of different clones from a primary HIV-1 culture. The supernatant fluid from the primary culture of PBMC from an HIV-1-infected individual was inoculated into MT-2 cells, PHA-activated PBMC, and Hu-PBL-SCID mice. After PCR amplification, the *env* sequences from a sample of the viruses that established infection in each of those environments were then determined. Derived Env amino acid sequences from those viruses are shown in Fig. 1. Because of synonymous nucleotide substitutions, these amino acid sequences do not completely mirror the nucleotide diversity present in the samples. However, two points of interest are apparent. First, two distinct subtypes of virus can be identified in the sequences amplified from the primary culture (labelled with the RT prefix): those characterized by the presence of an IKQR motif at positions 35 to 39 of the amplified Env sequence (RT-1, RT-7, RT-8, and RT-12) and those without this motif. Second, only those viruses carrying the IKQR motif grew in MT-2 cells and PBMC culture. The cultures from which these sequences were amplified uniformly demonstrated syncytium formation. Therefore, the viruses carrying this motif

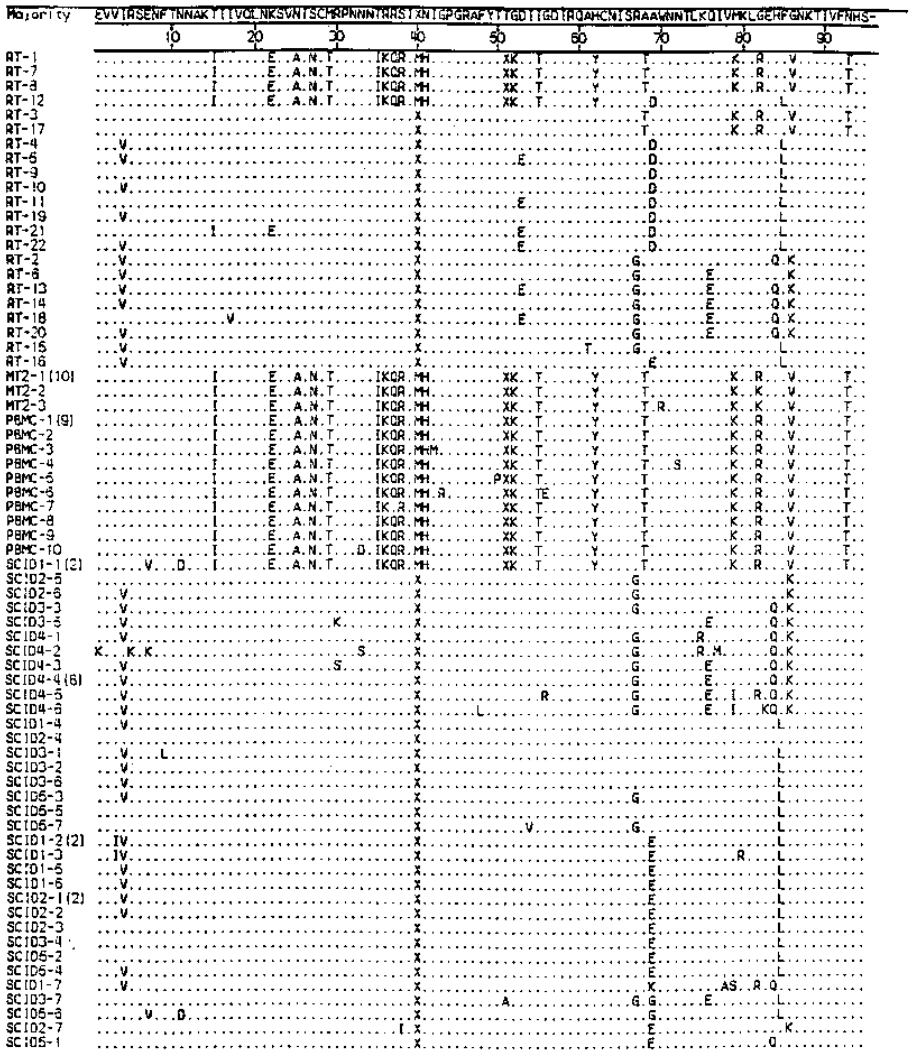

FIG. 1. Derived amino acid sequences from a region of the HIV-1 viral envelope that was amplified from different cell settings. The consensus sequence is displayed at the top, and amino acids that do not vary from the consensus at a given position are represented by dots. RT, sequences amplified from cDNA generated by reverse transcription of viral RNA from supernatant fluid of a primary culture; MT-2, sequences amplified from MT-2 cells inoculated with the primary culture supernatant fluid; PBMC, sequences amplified from PHA-stimulated normal PBMC inoculated with the primary culture fluid; SCID, sequences amplified from different Hu-PBL-SCID mice. The number following the cell type designation refers to the clone; "SCID" is followed by the mouse number and clone number.

were SI variants, while those that failed to grow in MT-2 cells and lacked the IKQR motif were likely to be NSI variants.

A phylogenetic network generated from the Env sequences is given in Fig. 2. With the initial focus on only the RT sequences (which represent a sample of the source population for the SCID, PBMC and MT sequences), the evolutionary tree is divided into two major branches or clades that are well differentiated by a minimum of 22 nucleotide substitutions of a total of 288 nucleotides and two insertions/deletions. The less diverse clade shown at the bottom of Fig. 2 consists of the SI RT sequences that share the IKQR motif; the more diverse top clade consists of the NSI variants. One sequence, RT-12, represents a recombinant between parental types in the SI and NSI clades.

As mentioned above, the RT sequences represent a sample of the population that was used to inoculate the MT-2, PBMC, and SCID cells. The fact that the RT sequences in this sample bracket almost all of the diversity observed in this phylogenetic tree indicates that the sampling was extensive enough to assess accurately the evolutionary affinities of all viruses that established infection in the MT-2, PBMC, and SCID environments. However, it still must be emphasized that the 22 RT sequences obtained represent only a sample of the inoculating population. Consequently, there are undoubtedly additional sequences in the RT population, and many of the successful inoculant sequences may well have been derived from RT sequences not present in the sample. Moreover, once inoculated into a cell line, the successful viruses can establish evolving lineages such that some of the diversity observed in the inoculant sequences may not be present in the original RT population. However, because the RT sample does span virtually the entire range of diversity observed in all sequences, we can legitimately identify the evolutionary affinities between the RT sequence population and the sequences obtained from viruses in the MT-2, PBMC, and SCID environments.

A nested cladistic categorical analysis was then executed to identify these evolutionary affinities, as described in Appendix. This analysis uses the evolutionary network of all the se-

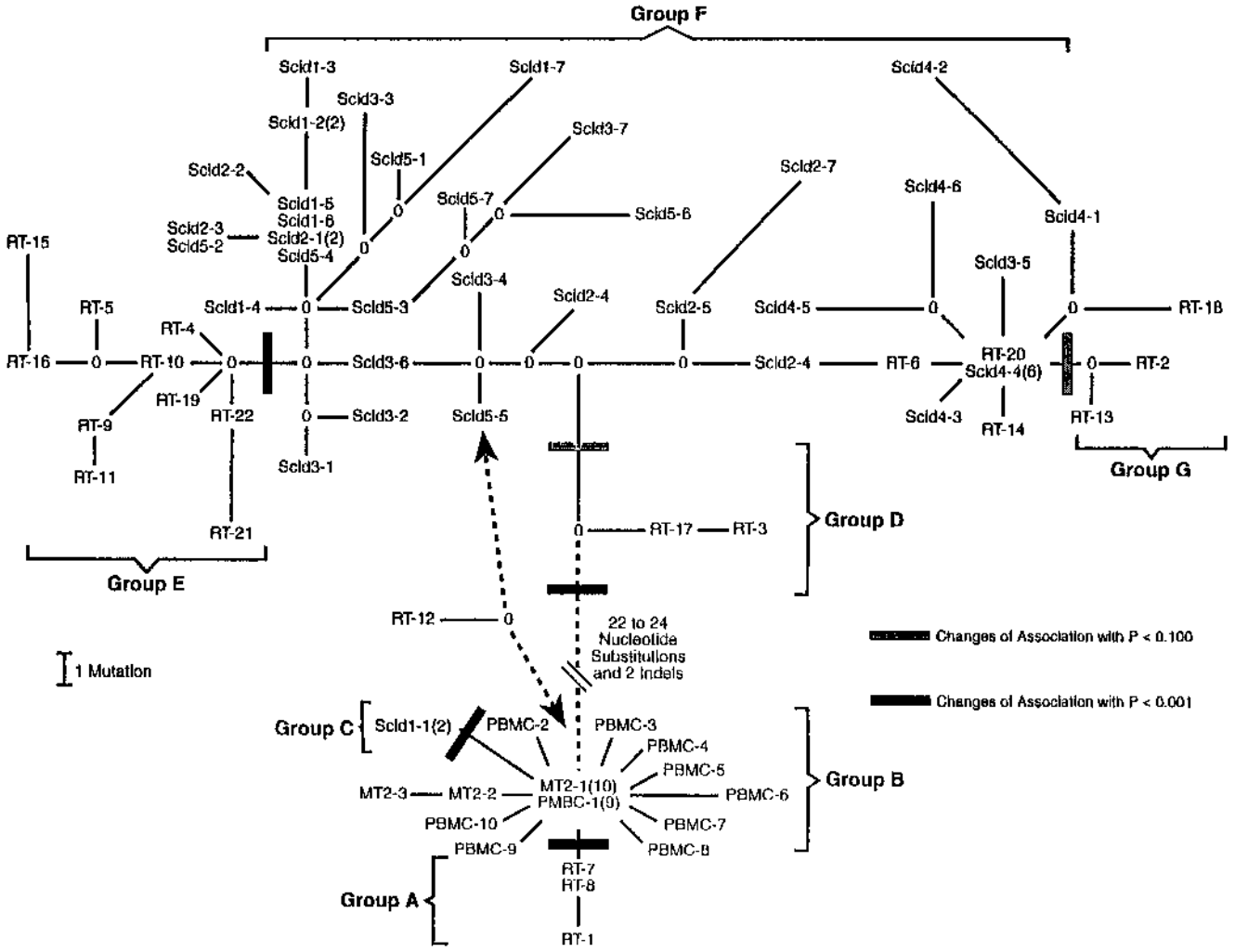

FIG. 2. Estimated evolutionary network of the HIV haplotypes. Haplotypes that are presented together as a block in the network have identical nucleotide sequences. In some cases, the same sequence was found more than once in the HIV clones isolated from a single tissue type or replicate. In these cases, the number of times the sequence was isolated from the sample is indicated in parentheses. Solid lines, branches whose length is expected to be proportional to the number of mutations in a parsimonious fashion, using the scale shown; dashed line, a branch that contains two insertions/deletions and a minimum of 22 nucleotide changes but that is likely to violate the principle of maximum parsimony. Only the maximum parsimony connection between the top and bottom halves of the network is indicated, but the dashed line could connect to either half within a single mutational change of the maximum parsimony connection. The arrows point to the portions of the network near the two parental types that yield the recombinant haplotype represented by RT-12. Bars, significant changes in association with haplotype categories.

quences as shown in Fig. 2 to define a nested statistical design. It is critical to note that this design is determined exclusively by the sequence data alone and therefore is completely unbiased with respect to tissue associations. After the nested design is defined from the sequence data, the observed tissue associations are overlaid upon the phylogenetic tree and statistical testing is performed to identify those evolutionary transitions or branches in the network that are associated with statistically significant changes in the tissue types from which the sequences were derived. A total of six large transitions in tissue associations were observed in this phylogenetic tree, as indicated by the heavy lines over specific branches in the phylogenetic network illustrated in Fig. 2. Four of these transitions were significant at the 0.001 level, and two were significant at the 0.100 level. These six major transitions in tissue associations divide the phylogenetic network into seven viral clusters (A to G), as summarized in Fig. 3.

It is apparent that viruses from the primary culture (RT) are widely distributed throughout the network and well represented in groups A, E, and G at the extremes of the tree. In contrast, the viruses that established infection in PBMC, MT-2 cells, and Hu-PBL-SCID mice are not randomly distributed throughout the tree. Instead, the virus sequences from each of those different cellular environments, with rare exception, cluster together tightly in individual regions of the tree. Of particular interest is the clustering of 40 of 42 (95%) of the sequences from the Hu-PBL-SCID mice in a single region of the NSI portion of the tree, indicating that not all NSI variants from the primary culture (the clones with the RT prefix) were equivalent in their abilities to establish infection in the mice.

The presence of all of the viral variants from PBMC and MT-2 cells within a single cluster (group B) also shows marked restriction of which viruses were transmitted in those settings. It also demonstrates that the cellular environment of activated PBMC favors selective transmission of the same viruses that are transmitted into the T-cell line MT-2. As indicated, these viruses all induced syncytia in the cultures in which they grew.

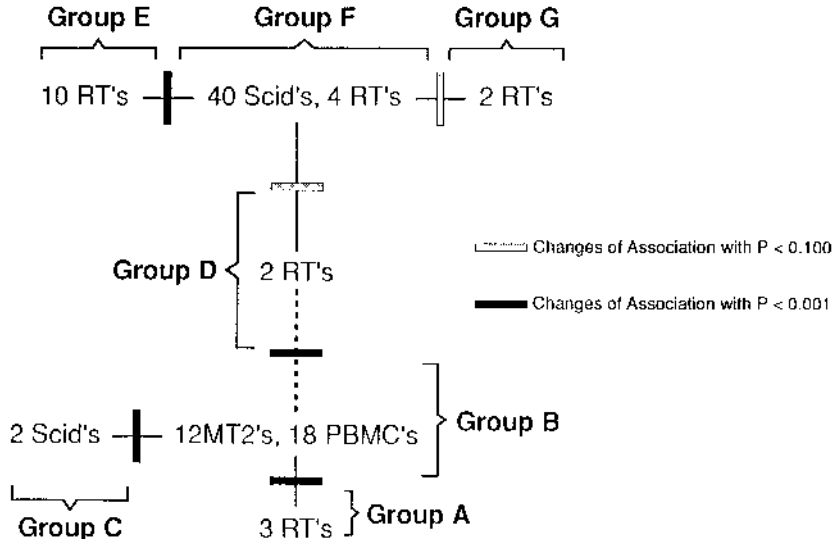

FIG. 3. Estimated evolutionary network of the HIV haplotypes showing only the portions of the network defined by significant transitions in association with cell type origin.

Activation state of human PBMC transplanted into Hu-PBL-SCID mice 8 days earlier. As previously noted, PBMC placed in culture are actively stimulated with PHA at the initiation of culture, while PBMC placed into Hu-PBL-SCID mice are not directly stimulated. One possible explanation, then, for the differences in the transmission pattern in Hu-PBL-SCID mice and that in PHA-stimulated PBMC would be a difference in the activation state of the human CD4 cells in the two settings. We examined in Hu-PBL-SCID mice the expression by CD4 T cells of HLA-DR, a class II major histocompatibility protein expressed on the surface of activated T lymphocytes (6, 7). Cells were subjected to flow-cytometric analysis 8 days after reconstitution. The proportions of CD4 T cells expressing HLA-DR in four mice were 5, 6, 9, and 14% (mean, 9%). A representative flow-cytometric analysis is shown in Fig. 4. This level of HLA-DR expression is very similar to that reported for $CD4^+$ T cells from freshly obtained HIV-1-negative donors (6, 7). In contrast to this finding, over 80% of T cells in stimulated PBMC tissue culture typically express this activation marker (7).

DISCUSSION

In the current study, the abilities of distinct HIV-1 variants to establish infection in PBMC depended on whether the PBMC were located in Hu-PBL-SCID mice or in standard PBMC tissue culture. A prototypic NSI HIV-1 variant, $HIV_{Ba\text{-}L}$, was more infectious in Hu-PBL-SCID mice than a prototypic SI variant, HIV_{MN}, but in PHA-stimulated PBMC tissue culture the SI variant was either equivalently infectious or more infectious, depending on the subject used as a source of PBMC. When PBMC tissue culture or Hu-PBL-SCID mice were inoculated with a primary isolate containing both SI and NSI variants, the SI variants exclusively established infection in tissue culture while the NSI variants predominated among viruses establishing infection in Hu-PBL-SCID mice. While, in general, it is certainly possible to infect PHA-activated PBMC with NSI variants of HIV-1, the required infectious dose may be higher than that which was present in our inoculum. We could, for example, establish infection in activated PBMC with $HIV_{Ba\text{-}L}$, but in the experiment shown in Table 1 a higher inoculum was required for this virus than for HIV_{MN}.

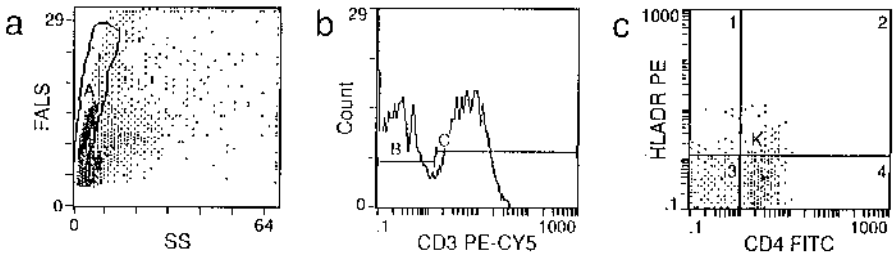

FIG. 4. Flow-cytometric analysis of data from mouse 4. (a) Forward (FALS) and 90° (SS) light scatter plot of peritoneal cells. Gate A includes lymphocytes. (b) Histogram of fluorescence of CD3 staining (horizontal axis) versus number of cells counted (vertical axis), gated on cells within gate A in the preceding panel. Region C indicates positive fluorescence for human CD3, i.e., human T cells, and included 47.7% of events in region A. (c) Two-dimensional histogram of CD4-FITC fluorescence (horizontal axis) versus HLA-DR–PE fluorescence. Quadrant 2 represents cells expressing both CD4 and HLA-DR; quadrant 4 represents cells expressing CD4 only. The dividing line between quadrants 2 and 4 was determined by using an isotype control antibody in combination with anti-CD4 antibody as described in Materials and Methods. The percentages of cells in quadrants 1 to 4 were 3.3, 6.6, 33.1, and 57.0%. Nonspecific binding of 0.4% was subtracted from the value in quadrant 2 to obtain the true percent of $CD4^+$ $HLA\text{-}DR^+$ cells in the peritoneal cells obtained from each mouse.

In addition, not all NSI variants from our primary virus inoculum appeared equally infectious in Hu-PBL-SCID mice. Those variants that established infection all segregated in a nonrandom manner within the same clade of the phylogenetic tree. Thus, the Hu-PBL-SCID mouse model demonstrated a pattern of restriction in the range of viruses transmitted similar to that observed clinically (14, 30, 31).

The viral variation in the Hu-PBL-SCID mice, although quite restricted, was greater than that in recently infected individuals, for whom less than 1% nucleotide sequence variation among isolates was seen (14, 30, 31). This could be because the range of variants to which an individual is exposed is narrower than that present in the inoculum used in these studies. Thus, the homogeneity observed among isolates in recently infected individuals may reflect both exposure to limited numbers of viral variants and selection for the variants that are most infectious.

The basis for the differences in viral selection in the PBMC in Hu-PBL-SCID mice and PHA-stimulated PBMC was not directly addressed in this study. However, the two environments studied clearly differ in degree of cellular activation, as reflected by the proportion of CD4 lymphocytes expressing the activation marker HLA-DR. It has been argued that cellular activation is essential for virus infection to proceed through reverse transcription and integration (1, 2, 29). The current data suggest that certain NSI variants may be better able to establish infection under conditions of low activation than are SI viruses. In support of this argument, it should be noted that in this study the level of HLA-DR expression by CD4 cells in the Hu-PBL-SCID mice was similar to that in human PBMC in vivo (12). The results with transmission of $HIV_{Ba\text{-}L}$ and $HIV\text{-}1_{MN}$ to Hu-PBL-SCID mice and the transmission of two apparent SI clones to Hu-PBL-SCID mice show that the restrictions on transmission are not absolute and can be overcome by larger viral inocula. Transmission of SI variants is, however, an infrequent occurrence in Hu-PBL-SCID mice, just as it is clinically (14, 30, 31).

Hu-PBL-SCID mice and PBMC tissue culture obviously differ by more than the state of activation of the human cells in the two systems, and it is possible that other factors may influence the observed differences in infectiousness of distinct HIV-1 variants. The possibility exists, for example, that the SCID mouse environment favors the persistence of clones of T cells that are selectively infected by specific subsets of the pool of HIV-1 variants. As the time from human-cell transplantation increases, the population of human T cells in the mice does become more oligoclonal in terms of more restricted antigen specificity (23). There is, however, no evidence for selection of HIV-1 variants on the basis of antigen specificity of T cells. Whether T-cell clones selected on other bases would preferentially favor infection with specific HIV-1 variants is unknown. Given the demonstrated importance of cell activation in productive infection and the gross difference in activation states between the two environments, we believe that this difference is the likely explanation for the patterns of HIV-1 infection in the two settings.

Tary-Lehman et al. reported that human T cells in Hu-PBL-SCID mice consisted of uniformly activated oligoclonal T-cell populations with specificity for mouse antigens (23). However, in that study PBMC from Hu-PBL-SCID mice were analyzed approximately 50 days postreconstitution with human cells, and the level of T-cell activation 8 days postreconstitution was not reported. The 8-day time point is important because that is when infection with HIV-1 is typically initiated. The lack of such early-time-point data in the previous studies may relate to the difficulty in identifying human cells among the mouse peritoneal cells before the human cell population has expanded. By removing a substantial proportion of the mouse cells from the peritoneal cells, we were able to identify and characterize the human cells in the mice at that early time point.

Mosier et al. reported that NSI variants of HIV-1 were more virulent in Hu-PBL-SCID mice than SI variants, i.e., they caused more rapid decline of the human $CD4^+$ T cells (18). This observation was unexpected because the appearance of SI variants in the clinical setting is usually associated with more rapid $CD4^+$ T-cell decline (9, 19). Our findings suggest a different explanation for the greater loss of T cells in Hu-PBL-SCID mice infected with NSI variants, namely, that those variants infected the mice with greater efficiency than the SI variants. If infection in Hu-PBL-SCID mice challenged with SI viruses occurs with low efficiency, then the viral load early after infection with SI viruses would be lower than that early after infection with NSI viruses. Thus, a more rapid CD4 T-cell decline in the mice challenged with NSI variants could simply reflect the greater viral load present shortly after inoculation in those mice, rather than an intrinsically greater cytopathic potential of NSI variants on a per-virion basis.

As mentioned above, the appearance of SI variants of HIV-1 in infected individuals is frequently associated with rapid progression to AIDS (9, 19). If the host environment plays an important role in selecting which viruses predominate, then the appearance of the virulent SI viral phenotype in the clinical setting could reflect a change in the host environment as well as viral mutation. Knowledge of how and why the host environment changes may provide important insights into HIV-1 pathogenesis and suggest new approaches to therapeutic intervention.

The effort to develop HIV-1 vaccines has been plagued by the heterogeneity of viral isolates. By understanding the importance of the cellular environment in selection of transmitted viruses, it should be possible to direct vaccine development at the more restricted range of viral variants likely to be involved in the spread of infection. The present results indicate that Hu-PBL-SCID mice may be useful for identifying and evaluating viral variants that should be studied as candidate vaccines.

APPENDIX

Tree estimation. An unrooted evolutionary tree of the observed unique sequences (haplotypes) was estimated by using the algorithm of Templeton et al. (25). The first step in this algorithm is to estimate the limits of parsimony. A Mathematica (27) package is available for calculating these limits and may be obtained by electronic-mail request to temple__a@biodec.wustl.edu. In this case, branch lengths less than eight mutational steps were determined to be parsimonious with a probability greater than 0.95 using equation 8 of Templeton et al. (25). This parsimony limit splits the haplotypes into two subsets separated by a branch of a minimum length of 22 mutational steps (Fig. 2), and the principle of maximum parsimony was used separately within these two subsets. However, even within this limit, the algorithm of Templeton et al. (25) is not equivalent to maximum parsimony alone. There were hundreds of equally parsimonious alternatives for the subset of haplotypes above the dashed line in Fig. 2. However, this algorithm first unites those haplotypes with the shortest mutational distances into the maximum parsimony network and then adds on those haplotypes that are more mutationally distant from all other haplotypes. This means that this algorithm disallows those parsimonious alternatives that assign additional mutational steps (due to convergent or parallel mutations) to the shorter branch lengths. Both parsimonious networks were completely resolved by this algorithm, as shown in Fig. 2. As mentioned above, the top and bottom parsimonious networks are separated by a branch of a minimum length of 22 nucleotide substitutions and two insertion/deletion mutations. Because there is a substantial probability that parsimony is violated in this case (up to two

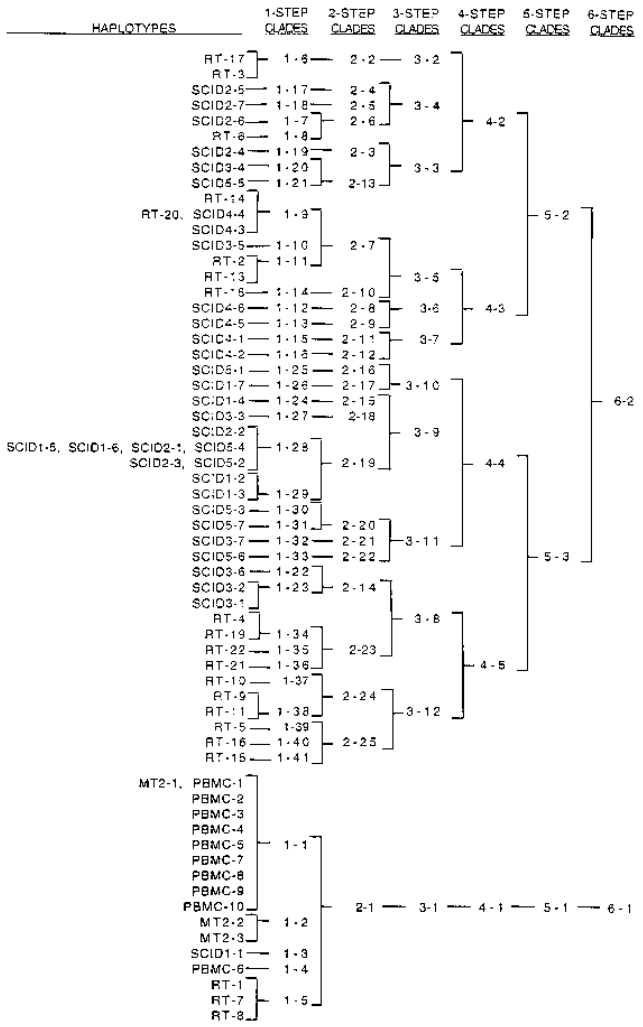

FIG. A1. Nested clades derived from the evolutionary network in Fig. 2.

additional mutations that represent repeat hits at the same site), there is some ambiguity about the exact connections between these two parsimonious networks. Fortunately, this ambiguity has no impact on the basic topology of the overall evolutionary tree and has no effect at all on the statistical analyses presented.

The algorithm of Templeton et al. (25) also searches for recombination, and the haplotype RT-12 was inferred to have arisen from recombination, as indicated by the dashed arrows in Fig. 2. One of the parental haplotypes (henceforth called PAR-1) differs by only a single nucleotide substitution from the sequence shared by MT2-1 and PBMC-1, at least in the region of nucleotide positions 1 to 201. That single nucleotide difference had already been inferred to occur on the long branch in Fig. 2 leading to MT2-1/PBMC-1 regardless of the inference of a recombination event. The other parental sequence is identical to SCID5-5, at least at nucleotide positions 185 to 288. Between positions 1 to 184 inclusive, RT-12 shares with PAR-1 18 nucleotide substitutions and two insertions/deletions that differentiate both of these sequences from SCID5-5; between positions 202 to 288 inclusive, RT-12 shares with SCID5-5 seven nucleotide substitutions that differentiate both of these sequences from PAR-1. Between nucleotide positions 185 to 201 inclusive, all three sequences are identical, and the putative recombination event must have occurred within this interval.

Categorical associations. To see if the haplotypes were nonrandomly associated with the various cell types, a nested categorical association of cell type origin versus position in the haplotype evolutionary network was executed by using the testing procedure described by Templeton and Sing (26). This test first converts the evolutionary network into a set of nested categories that represent larger and larger branches (clades) of the haplotype network. Accordingly, haplotypes were nested into one-step clades, one-step clades were nested into two-step clades, etc., by using the nesting rules described by Templeton et al. (24). The resulting nested categories are given in Fig. A1. Associations were then examined between these nested clades and the following categories: RT, MT2, PBMC, and SCID. The null hypothesis of no association was tested by repeated evaluation of a contingency chi-square-type statistic using 1,000 random permutations of the data that preserve marginal values, as outlined by Templeton and Sing (26). Only those nested categories that have variation in both clades and tissue categories are informative about when transitions in association occur, and the test results are given in Table A1. Because of small sample sizes, many of the nesting categories, particularly at the lower nesting levels, could not even in principle yield significant results at the 5% level, so to inspect for biological patterns, any test yielding a probability of 10% or less was regarded as biologically significant. As can be seen in Table A1, six nesting clades yielded significant results at the 10% level or lower. For three of these six nesting clades, there were only two nested clades within a nesting category, so the significant change in association could be localized on the evolutionary network as being the branch connecting the two contrasted clades. However, in the other three cases, there were multiple evolutionary branches within the nested category. In order to localize the overall clade effect, the

TABLE A1. Results of the nested, permutational analysis using the nested design in Fig. A1 and based on 1,000 random permutations for each nested group tested[a]

Clades tested, nesting clade	Permutation probability
Haplotypes, 1-1	1.000
Haplotypes, 1-9	0.500
1-step clades, 2-1	0.000
1-step clades, 2-6	1.000
1-step clades, 2-7	0.082
2-step clades, 3-4	1.000
2-step clades, 3-5	0.440
2-step clades, 3-8	0.019
3-step clades, 4-2	0.098
3-step clades, 4-3	0.330
3-step clades, 4-5	0.220
4-step clades, 5-2	1.000
4-step clades, 5-3	0.000
5-step clades, 6-2	1.000
6-step clades, entire network	0.000

[a] Only nonredundant clades having more than one category type can be tested.

TABLE A2. Localization of significant effects within nesting clades containing more than two nested clades

Nesting clade contrast	Permutation probability or FET[a]
2-1	
1-1 vs 1-2	0.155
1-1 vs 1-3	0.001
1-1 vs 1-4	0.576
1-1 vs 1-5	0.000
2-7	
1-9 vs 1-10	0.800
1-9 vs 1-11	0.100
4-2	
3-3 vs 3-2	0.100
3-3 vs 3-4	0.571

[a] FET, Fisher's exact test.

individual evolutionary branches were tested in a pairwise fashion. The results are shown in Table A2. As can be seen, the significant effect observed within nesting clade 2-1 actually is associated with two strong transitions of associations. Within nesting clades 2-7 and 4-2, both significant overall at the 10% level, only one contrast within each was significant at the 10% level Fisher's exact test.

As discussed by Templeton et al. (24), significant results on adjacent branches in the haplotype network need to be inspected further because of spillover effects; that is, a strong association at one level of nesting may affect a contrast at a different level as well. Of the seven branches associated with significant changes in association at the 10% level, two pairs are on adjacent branches. The first pair involves the significant effects localized in clades 3-8 and 5-3. The branch separating the two nested clades within 3-8 (2-14 and 2-23) is associated with a large change from an exclusively SCID clade (three SCID haplotypes are in 2-14) to an exclusively RT clade (four RT haplotypes are in 2-23). The significant effect observed in clade 5-3 is also a transition from an exclusively SCID clade (4-4 with 19 SCID haplotypes) to a nearly exclusively RT clade (4-5 with 10 RT haplotypes and 3 SCID haplotypes). The SCID haplotypes found in 4-5 are the same three SCID haplotypes found in 2-14, so this is clearly a spillover effect. By moving 2-14 into 4-4, the contrast is strengthened, yielding an exclusively SCID branch (2-14 plus 4-4) with 22 haplotypes and an exclusively RT branch (3-12) with 10 haplotypes (significant at the 0.0000 level with Fisher's exact test). Hence, this dramatic SCID-to-RT change in association occurs upon a single branch in the haplotype network as identified in clade 3-8 but is so strong that it spilled over into the 5-3 test result.

The other potential spillover effect is with the pair 4-2 and the entire cladogram (that is, the contrast of clade 6-1 versus clade 6-2). However, the 4-2 result is a SCID-to-RT transition, whereas the other branch (the dashed branch in Fig. 2) is an RT-to-MT2/PBMC transition. Hence, the biological categories involved in these significant results are quite different, so these are not spillover effects.

Because of the spillover effect observed with the 3-8–5-3 pair, the seven significant transitions are reduced to six. The locations of these transitions and their statistical strengths are indicated by the bars in Fig. 2. Figure 3 shows a summary of the haplotype composition in the different parts of the evolutionary network defined by these transitions.

ACKNOWLEDGMENTS

This work was supported by Public Health Service grants DA09717, DA04334, DA09541, AI32376, and AI35525.

We thank Gene Barbour, Zhe Wang, Zheng Chen, and Karen Chadwick for expert technical assistance.

REFERENCES

1. **Bukrinsky, M. I., N. Sharova, M. P. Dempsey, T. L. Stanwick, A. G. Bukrinskaya, S. Haggerty, and M. Stevenson.** 1992. Active nuclear import of human immunodeficiency virus type 1 preintegration complexes. Proc. Natl. Acad. Sci. USA **89:**6580–6584.
2. **Bukrinsky, M. I., T. L. Stanwick, M. P. Dempsey, and M. Stevenson.** 1991. Quiescent T lymphocytes as an inducible virus reservoir in HIV-1 infection. Science **254:**423–427.
3. **Crandall, K. A.** 1995. Intraspecific phylogenetics: support for dental transmission of human immunodeficiency virus. J. Virol. **69:**2351–2356.
4. **DeBry, R. W., L. G. Abele, S. H. Weiss, M. D. Hill, M. Bouzas, E. Lorenzo, F. Graebnitz, and L. Resnick.** 1993. Dental HIV transmission? Nature **361:** 691.
5. **Delwart, E. L., H. W. Sheppard, B. D. Walker, J. Goudsmit, and J. I. Mullins.** 1994. Human immunodeficiency virus type 1 evolution in vivo tracked by DNA heteroduplex mobility assays. J. Virol. **68:**6672–6683.
6. **Evans, R. L., T. J. Faldetta, R. E. Humphreys, D. M. Pratt, E. J. Yunis, and S. F. Schlossman.** 1978. Peripheral human T cells sensitized in mixed leukocyte culture synthesize and express Ia-like antigens. J. Exp. Med. **148:** 1440–1445.
7. **Hercend, T., J. Ritz, S. F. Schlossman, and E. L. Reinherz.** 1981. Comparative expression of T9, T10, and Ia antigens on activated human T cell subsets. Hum. Immunol. **3:**247–259.
8. **Holmes, E. C., L. Q. Zhang, P. Robertson, A. Cleland, E. Harvey, P. Simmonds, and A. J. Leigh Brown.** 1995. The molecular epidemiology of human immunodeficiency virus type 1 in Edinburgh. J. Infect. Dis. **171:**45–53.
9. **Koot, M., I. P. Keet, A. H. Vos, R. E. de Goede, M. T. Roos, R. A. Coutinho, F. Miedema, P. T. Schellekens, and M. Tersmette.** 1993. Prognostic value of HIV-1 syncytium-inducing phenotype for rate of CD4+ cell depletion and progression to AIDS. Ann. Intern. Med. **118:**681–688.
10. **Korber, B., S. Wolinsky, B. Haynes, K. Kunstman, R. Levy, M. Furtado, P. Otto, and G. Myers.** 1992. HIV-1 intrapatient sequence diversity in the immunogenic v3 region. AIDS Res. Hum. Retroviruses **8:**1461–1465.
11. **Lukashov, V. V., C. L. Kuiken, and J. Goudsmit.** 1995. Intrahost human immunodeficiency virus type 1 evolution is related to length of the immunocompetent period. J. Virol. **69:**6911–6916.
12. **Mahalingam, M., M. Peakman, E. T. Davies, A. Pozniak, T. J. McManus, and D. Vergani.** 1993. T cell activation and disease severity in HIV infection. Clin. Exp. Immunol. **93:**337–343.
13. **Maniatis, T., E. F. Fritsch, and J. Sambrook.** 1982. Molecular cloning: a laboratory manual. Cold Spring Harbor Laboratory, Cold Spring Harbor, N.Y.
14. **Markham, R. B., X. F. Yu, H. Farzadegan, S. Ray, and D. Vlahov.** 1995. HIV-1 env and p17 gag sequence variation in polymerase chain reaction positive, seronegative injection drug users. J. Infect. Dis. **171:**797–804.
15. **McNearney, T., Z. Hornickova, B. Kloster, A. Birdwell, G. A. Storch, S. H. Polmar, M. Arens, and L. Ratner.** 1993. Evolution of sequence divergence among human immunodeficiency virus type 1 isolates derived from a blood donor and a recipient. Pediatr. Res. **33:**36–42.
16. **Mosier, D. E., R. J. Gulizia, S. M. Baird, and D. B. Wilson.** 1988. Transfer of a functional human immune system to mice with severe combined immunodeficiency. Nature **335:**256–259.
17. **Mosier, D. E., R. J. Gulizia, S. M. Baird, D. B. Wilson, D. H. Spector, and S. A. Spector.** 1991. Human immunodeficiency virus infection of human-PBL-SCID mice. Science **251:**791–794.
18. **Mosier, D. E., R. J. Gulizia, P. D. MacIsaac, B. E. Torbett, and J. A. Levy.** 1993. Rapid loss of CD4+ T cells in human-PBL-SCID mice by noncytopathic HIV isolates. Science **260:**689–692.
19. **Nielsen, C., C. Pedersen, J. D. Lundgren, and J. Gerstoft.** 1993. Biological properties of HIV isolates in primary HIV infection: consequences for the subsequent course of infection. AIDS **7:**1035–1040.
20. **Ou, C. Y., C. A. Ciesielski, G. Myers, C. I. Bandea, C. C. Luo, B. T. M. Korber, J. I. Mullins, G. Schochetman, R. L. Berkelman, A. N. Economou, J. J. Witte, L. J. Furman, G. A. Satten, K. A. MacInnes, J. W. Curran, H. W. Jaffe, L. I. Group, and E. I. Group.** 1992. Molecular epidemiology of HIV transmission in a dental practice. Science **256:**1165–1171.
21. **Sanger, F., S. Nicklen, and A. R. Coulson.** 1977. DNA sequencing with chain-terminating inhibitors. Proc. Natl. Acad. Sci. USA **74:**5463–5467.
22. **Tary-Lehmann, M., P. V. Lehmann, D. Schols, M. G. Roncarolo, and A. Saxon.** 1994. Anti-SCID mouse reactivity shapes the human CD4+ T cell repertoire in hu-PBL-SCID chimeras. J. Exp. Med. **180:**1817–1827.
23. **Tary-Lehmann, M., and A. Saxon.** 1992. Human mature T cells that are anergic in vivo prevail in SCID mice reconstituted with human peripheral blood. J. Exp. Med. **175:**503–516.
24. **Templeton, A. R., E. Boerwinkle, and C. F. Sing.** 1987. A cladistic analysis of phenotypic associations with haplotypes inferred from restriction endonuclease mapping. Genetics **117:**343–351.
25. **Templeton, A. R., K. A. Crandall, and C. F. Sing.** 1992. A cladistic analysis of phenotypic associations with haplotypes inferred from restriction endonuclease mapping and DNA sequence data. III. Cladogram estimation. Genetics **132:**619–633.
26. **Templeton, A. R., and C. F. Sing.** 1993. A cladistic analysis of phenotypic associations with haplotypes inferred from restriction endonuclease mapping. IV. Nested analyses with cladogram uncertainty and recombination. Genetics **134:**659–669.
27. **Wolfram, S.** 1991. Mathematica. Addison-Wesley, Redwood City, Calif.
28. **Wysocki, L. J., and V. L. Sato.** 1978. "Panning" for lymphocytes: a method for cell selection. Proc. Natl. Acad. Sci. USA **75:**2844.
29. **Zack, J. A., S. J. Arrigo, S. R. Weitsman, A. S. Go, A. Haislip, and I. S. Y. Chen.** 1990. HIV-1 entry into quiescent primary lymphocytes: molecular analysis reveals a labile, latent viral structure. Cell **61:**213–222.
30. **Zhang, L. Q., P. MacKenzie, A. Cleland, E. C. Holmes, A. J. Leigh Brown, and P. Simmonds.** 1993. Selection for specific sequences in the external envelope protein of human immunodeficiency virus type 1 upon primary infection. J. Virol. **67:**3345–3356.
31. **Zhu, T., H. Mo, N. Wang, D. Nam, Y. Cao, R. A. Koup, and D. D. Ho.** 1993. Genotypic and phenotypic characterization of HIV-1 in patients with primary infection. Science **261:**1179–1181.